Mineralogical and chemical investigations on the ceramic technology in Čoġā Zanbil, (Iran, 1250 B.C.)

Mohammadamin Emami[1,*] and Reinhard Trettin[2]

[1]Faculty of Conservation, Art University of Isfahan, P.O. Box 1744, Isfahan, Iran
[2]Institute for building- and materials chemistry, University of Siegen,
Paul Bonatz Str. 9-11, D-57068 Siegen, Germany
[*]Corresponding author: *emami@chemie.uni-siegen.de*

Abstract

Characterizations of archaeological finds are an essential feature for the interpretation of data from excavations. The investigated samples date from Elam period (1250 B.C.), which is an important period for archaeology, because of the introduction of new technologies that ameliorate the quality of materials used in daily life, and furthermore because of the expansion of the Elamite kingdom in the Iranian plateau.

Basically this paper focused on the investigation of the parameters which have been interested for characterizing the ceramics production in the past.

The ceramic pieces studied in this paper come from archaeological excavations carried out in Čoġā Zanbil, in the south west of Iran, between 2002 and 2004. Based on archaeological interpretation they belong to the middle Elamite period (1500-1100 B.C.).

The samples have been investigated by quantitative X-ray diffraction inclusive Rietveld phase refining method for determining the crystalline phases in the matrix of ceramics, and simultaneous thermo analysis to characterize the decomposition of the constituent phases during the sintering process. Furthermore thermo analytical studies proved that, during the middle Elamite period, existed a dissimilar thermal behaviour due to different fabrication conditions. Observation by polarized light microscopy included additional information on the manufacturing process by means of the identification of different additives, used within the ceramic matrix.

The results provided information on the existence of a similar raw material, and different manufacturing technique in the ceramic production in the middle Elamite period, in Čoġā Zanbil.

Key words: Archaeometry; Ceramic; Powder Diffraction; Rietveld Method; Simulated Thermo Analysis; Polarized Light Microscopy; Elamites; Čoġā Zanbil; Iran.

Introduction

The southwest of Iran - an area not far from the domains of the Zagros Mountains, between two large rivers named Karoon and Dez - is the birth place of the great kingdom of Elam in ca. 4000 B.C. (Potts, 1999). This region is located in ca. 90 km north of the city Ahvaz and 35 km south of the ancient city of Susa (Figure 1). In the mid-14th century, the southern district of the Susiana plain was elected as capital of Elam by king "Untsh Gal". He ordered to build a holy capital called "Dor Untash" as a pilgrimage centre. Today, this holy city is known as Čoġā Zanbil (Figure 2), and is located 25 km from the residential place, Haft Tappeh (Ghirshman, 1968, Negahban, 1991). Čoġā Zanbil is an important archaeological site in the Susiana plain and it is dated to the Elamite period due to the archaeological finds. The archaeological documentation on this area goes back to reports, written in 1962 by R. McCormik Adams. Excavations in Čoġā Zanbil and in the periphery of the city began in autumn 1966, and were directed by Grishman (1968).

According to the archaeological interpretations based on the stylistic features of finds such as ceramics and architectural foundations, the Elamite period is divided into four sub-periods (Potts, 1999):

(I)   Proto- Elamite (4000 - 2500 B.C.)
(II)   Early Elamite (2500 - 1500 B.C.)
(III)   Middle Elamite (1500 - 1100 B.C.)
(IV)   The recent Empire (750 - 640 B.C.)

Čoġā Zanbil is not only important as the religious periphery of the Elam dynasty, but in the ancient world it was also a technical centre for the production of bronze objects, as well as of binding material, ceramics and bricks (Emami, 1996; Emami et al., 2008; Oudbashi and Emami, 2010). According to archaeological evidence and geological settings in the region, the settlements had once great potentialities in the use of soil and natural resources in the vicinity, where they could gather the best quality minerals. Clay, calcareous stone, gypsum and granite outcrops are among the most important natural resources that would also contribute to agricultural activities in this part of the Susiana plain. The soft bituminous stones were really a gift for the civilian of Susiana and Mesopotamia (Le Chatelier, 1912). The data suggest that the rivers were the most important paths for transferring technology and trading science (Sumner, 1972).

Ancient ceramic artefacts are among the most interesting objects to study the relationship between man and environment. Indeed, every piece of pottery is an open book on its manufacturing process and on its history (Maggetti and Schwab, 1982). The objects which are being investigated here, can be distinguished by their differences in shape and colour as well as in their matrix. Based on the archaeological observation and reports carried out in this field, pottery is the most commonly found everyday product, often catalogued in enormous quantity. Archaeological investigations have been carried out for some years, but the analytical evaluations of archaeological finds from this area are a recent investigation.

Ancient pottery is described as an object with a high porosity and a clayey matrix with either different or similar kinds of mixtures with a glassy matrix (Salmang and Scholze, 1983). For an archaeometrically oriented mineralogist, pottery is manufactured by means of different pyrotechnological processes. The most interesting questions are: how long does the craftsman or potter use the same manufacturing process or similar raw materials? If there was any challenge, which kind of technical highlights can be identified by investigations?

For this study different analytical approaches have been used for the characterization of ceramics from Čoġā Zanbil (1500-1100 B.C.). Classifying ceramics involves the understanding

of the different manufacturing process, used during a well-known historical period with respect to their raw materials and manufacturing processes. After the characterization of ceramic, the study of the manufacture and the performance of ceramics residues, the focus is now on the development of manufacturing techniques of pottery dated to the time between 1250 and 700 B.C., discovered in the excavations in 2004.

The ceramic remains considered here showed different shapes and style as well as different physical and chemical properties, depending on their structure and constituent minerals, expected in some investigated ancient ware from Mesopotamia (Noll, 1990). Models for the investigation on potteries have for a long time been focussed on research carried out by different authors (Emami and Trettin, 2010). The

archaeological evidence on Čoġā Zanbil is published in various reports, but these may in part reflect theoretical concepts that do not match laboratory results. In this paper the results of scientific analysis of ceramic remains are outlined.

Application of quantitative x-ray diffraction with Rietveld refining method and themo-analysis have discussed on the ceramics from Persepolis, Iran (Emami et al., 2011). These models take into account the different methodological path in the resource-rich of ancient civilizations (Maggetti et al., 2011). In this paper, the beginnings of the production of ceramics in south west of Iran will be put together with a cursory overview of the characterization of ceramic pieces. By synthesizing data from a number of current research projects, exploring the usage of

Figure 1. Map showing the location of sites and nearby roads and cities.

Figure 2. Temple of Čoġā Zanbil built by Untash Gal in 1250 B.C.

mineralogical data for interpreting of ancient objects (Drebushchak et al., 2011; Szilagyi et al., 2012).

Geological setting

The geological setting is important for understanding the geological- and mineralogical development of the earth through time. Morphological and geological features in this region demonstrate it to be a field with typical complex structures including geosynclinals and new marine sedimentation in the south west of Iran, close to the Iraqi border. This setting caused essential occurrences on the raw materials through out of geological process, and their outcrops on the earth, in different facies (Tehrani, 1989). Erosion can be seen all around the Khuzestan province and occurs in different formations on the ground. River streams, underground irrigation, hot and dry weather, thaw-freezing effects and salt recrystallization are the main effects causing corrosion in the Khouzestan province and mainly around the Čoġā Zanbil complex (Bullard, 1970).

The Iranian plateau is affiliated with the upduction of Former Ocean Tethys in 190 million years ago and, accordingly, it is expected to have mainly outcrops consist of biochemical and marine carbonate sediments (Van der Voo,

1993). There are three important formations which are responsible for the geological setting of this area: The Agha-Jari formation, the Lahbari formation and the Quaternary formation. The entire sedimentary sequences are illustrated in Table 1.

Agha-jari consists of red-grey sandstone and greywacke, and the chemical variation depends from the Fe^{3+}/Al^{3+} ratios in its sandstone. Such melange outcrops are interpreted as high subduction erosion on the surface (Gradstein et al., 2004). The Agha-Jari formation consists of gypsum and mergel which became visible in calcareous formation as well as chertarnite. The sedimentation facies, classified from early time to the recent period, include (I) mergel sand stone (M-Pla^{ms}), (II) Conglomerate (M-Pla^{c}) and (III) recent sandstone with conglomerate (M-Pla^{sc}).

The Lahbari formation consist mainly of calc-arnite, limestone, silt and fine granular sandstone, followed by a thin layer of gypsum and mergel, above which there is alluvial sedimentation (Fesharaki et al., 2007). The Lahbari formation is classified by two sub layers on this field: (I) early Lahbari (Pl$^{1}_{la}$) and (II) recent Lahbari (pl$^{2}_{la}$).

The quaternary formation outcrops are common on this field and surrounded Čoġā Zanbil, but were very rapidly eroded. The mineralogical sequences contain silt, sand and

Table 1. Related geological time scale on the field.

Period			Symbol	
Quaternary	Holocene		Q_{al}	New alluvial sediments consist of sand, silt and gravel.
			Q_{14}	Alluvial sediments with sand silt and clay with the remains of corroded material from the building.
			Q_{13}	Accumulation of new alluvial sediments consists of fain stone agglomerate, sand and gypsum.
			Q_{la}	Secondary sedimentation of gypsum and sand.
			Q_{12}	Accumulation of new compact sediments wich consists of granular stone aggregates.
			Q_{11}	Old standing alluvial sediments consist of conglomerates and granular sand.
Tertiary	Neogene	Miopalaeogene	PL^2_{la}	Recently weathering consists of sand, conglomerate and clay.
			PL^1_{la}	Exchangeable layers between gypsum and sand.
			M-PLG	Sedimpation of greyish sand and clay with gypsum.

clay. This setting is also responsible for a clayey reservoir on the field. The Quaternary contains five sublayers; (I) old tercier (Q^{t1}), (II) jung tercier (Q^{t2}), (III) weathered layer (Q^5), (IV) recent tercier (Q^{t3}) and (V) recent alluvial sediments (Q^{t4} - Q^{al}). The lithological data proved that in this sequence conglomerates consist of granular quartz sandstone, cemented with a calcareous matrix. Granular sandstones are not well rounded due to their nearness to the original sources.

Recently alluvial sedimentation is mainly observed near the temple and it is forming till today (Malek-Abbasi, 2004). Salt recrystallization and salt pillars denseness around Čoġā Zanbil suggest typical marine evaporate on the field that followed by metamorphose. In the external part of the soil cloride enrichment as $MgCl_2$ composition appeared in some accumulation texture on the field. High carbonate enrichment is caused by evaporation of seawater. The formation in a thin layer consists of gypsum. Anhydrite was

expected, because of the evaporation of carbonate in an arid climate with sulphate constituents.

The best sedimentation sequences are observed in the water canals close to the temple. According to the strata formation, the Q^{t4} and Q^{al} are both the main sediments around Čoġā Zanbil. These two sequences have the same old standing but different lithological-mineralogical constituents.

Material and Methods

Samples Description

Thirty five samples (ceramic pieces) from surface excavation as well as archaeological excavation have been selected, with special attention to their morphology, surface character and textural property. The objects are supposed to have been produced in Čoġā Zanbil and they were sampled because of the reasonable attribution to this field. The samples have been archaeologically and iconographically studied, and because of their stylistic features their provenance from Čoġā

Zanbil has been accepted (Mofidi Nasrabadi, 2003). The investigated samples are mainly dated to the middle Elamite period (15th B.C.) and show a great variety with respect to their functionality. The ceramics are mostly vases, bowls, jugs and plates.

Chronologically, the ceramics dated to 250 BC are the earliest found in Čoġā Zanbil. The shapes of these objects are mostly similar, but their color varies considerably from white (8/2) to bright olive-green (6/3) to reddish-yellow (6/8) yellow (8/6) and pink (7/4), based on the Munsell table of color. The effect of straw (organic additives which have been used to clayey raw materials) can also be observed on the surface. The ceramic pieces have been selected as relevant samples, belonging to the same range of dating (1500 to 1100 B.C.) (Mofidi Nasrabadi, 2003; Malek-Abbasi, 2004). Classification of the samples according to their applications and their related dating are described in the Table 2. To get a good overview to the samples, macroscopical illustrations of some pieces are shown in the Figure 3.

Analytical Methods

The investigation of the ceramic samples has been carried out by following some criteria that must be taken into account in the interpretation and characterization of samples:

(I) the consistency of the matrix for the interpretation of mechanical properties of ceramic matrices (Wong and Buenfeld, 2006);

(II) the characterization of the binding material by means of clayey-, calcareous- and organic based materials, that was also recognized as part of the matrix as fine-, crude and colloidal matrix (Maggetti and Schwab, 1982);

(III) the characterization of the mineralogical constituents for interpreting the raw material processing as well as the development of the firing technology and the surface modification of ancient products (Martineau et al., 2007, Emami et al., 2008).

35 samples have been analysed by X-ray fluorescence (Bruker® spectra plus 2008 software), for the determination of the bulk chemical composition of the ceramic matrix. The major, minor and trace elements measured as oxides, and the correlation between the main oxide constituents tend to allow a good classification of the ceramics (Noll, 1991). Qualitative X-ray diffraction has been used for determining the crystalline phase compositions (QXRD, from PANalytical, X'pert PRO and the X'pert high© Score software, Cu-Kα, 40 kV, 40 mA, measuring time 1 sec per step). All crystallographic parameters of phases have been refined with the Rietveld refining method in order to get a better crystal structure description of the phases. Crystallographic structure fitting emphasised the quality of the goodness of the fitting factor, i.e. the minimum shifting between calculated and measured diffractograms by Rietveld method (Emami, 2008). Simultaneous thermo-analysis (STA, from NETZSCH, STA 449C Jupiter, and Proteus Analysis Software Version 4.8) achieves superior results in the determination of the firing temperature as well as in the phase decomposition during the firing process (Emami et al., 2008). Polarized light microscopy is a complimentary method for the petrological - petrographical observation of the crystalline phase constituents, carried out with an Olympus, BX 51 instrument with AnalySIS five pictures Software.

Results and discussion

Chemical composition of ceramics in the (CaO+MgO) - SiO$_2$ - Al$_2$O$_3$ system

The result of the XRF analysis on the ternary system (CaO+MgO) - SiO$_2$ - Al$_2$O$_3$ proved that the pottery from Čoġā Zanbil has to be classified as calcium rich, till high calcium-rich ceramic (Noll, 1991; Emami, 2008) (Figure 4, Table 3). According to the (CM)SA diagram the results concentrated in the quartz - diopside - anorthite line, based on the usage of mostly calcareous raw

Table 2. Classification and description of samples according to their applications.

Application	Description No.	Archaeological Dating
Čoġā Zanbil		
	C.Z. 81-15,2-7	
	C.Z. 80-725-293	
Plate	C.Z. 81-653-182	1100 – 1200 B.C.
	C.Z. 81-588c-325	1100 – 1200 B.C.
	C.Z. 80-652-80	900 – 1000 B.C.
	C.Z. 81-19-67	900 – 1000 B.C.
Big Jugs	C.Z. 80-16-6	900 – 1000 B.C.
Big open Jugs	C.Z. 81-14-12	1100 – 1200 B.C.
	C.Z. 81-588c-338	1100 – 1200 B.C.
	C.Z. 80-720-161	900 – 1000 B.C.
	C.Z. 80-14-35	900 – 1000 B.C.
	C.Z. 80-14-42	900 – 1000 B.C.
	C.Z. 80-14-44	900 – 1000 B.C.
	C.Z. 80-16-8	900 – 1000 B.C.
	C.Z. 81-588c-502	
	C.Z. 81-588c-382	900 – 1000 BC.
	C.Z. 81-588c-349	900 – 1000 B.C.
	C.Z. 81-19-85	900 – 1000 B.C.
	C.Z. 81-653-175	700 – 800 B.C.
Bowl	C.Z. 80-14-36	1100 – 1200 B.C.
	C.Z. 80-16-17	1100 – 1200 B.C.
	C.Z. 80-725-437	900 – 1000 B.C.
	C.Z. 80-628-2	900 – 1000 B.C.
	C.Z. 81-588c-510	900 – 1000 B.C.
	C.Z. 80-628-48	900 – 1000 B.C.
	C.Z. 81-588c-306	900 – 1000 B.C.
	C.Z. 80-725-282	700 – 800 B.C.
	C.Z. 80-652-131	700 – 800 B.C.
	C.Z. 81-724-61	700 – 800 B.C.
Pitcher	C.Z. 81-588c-254	900 – 1000 B.C.
	C.Z. 80-725-288	900 – 1000 B.C.
	C.Z. 80-725-306	900 – 1000 B..C.
Cup	C.Z. 81-640-4	700 – 800 B.C.
	C.Z. 80-640-56	700 – 800 B.C.
Beaker	C.Z. 80-627-148	700 – 800 B.C.

materials. The distribution of the results of bulk chemical analysis in this area illustrate that the results are not clustered in a separated areas, but also that they are scattering toward the quartz – calcite line, interpreted as essential for choosing the raw materials from 1200 till 700 B.C. (Emami et al., 2008). The distribution indicates that the raw materials seem to be dissimilar in the passing of time. As shown by the calcium constituent from calcareous materials in the samples, the objects from Čoġā Zanbil are more or less analogous to the ceramics from other

Table 3. Bulk chemical analysis of the samples. Major elements in wt% and minor elements in ppm.

Samples	SiO$_2$	TiO$_2$	Al$_2$O$_3$	Fe$_2$O$_3$	MnO	MgO	CaO	Na$_2$O	K$_2$O	P$_2$O$_5$	SO$_3$	Cl
					wt%							
CZ. 80-14-35	46.37	0.77	12.20	6.34	0.09	4.64	16.05	0.83	2.56	0.17	0.59	0.05
CZ. 81-653-175	54.92	0.76	12.20	6.40	0.07	4.47	10.62	1.26	2.73	0.64	0.20	0.04
CZ. 80-725-293	41.42	0.63	10.20	5.69	0.09	4.18	20.38	0.60	2.25	0.23	0.46	0.06
CZ. 80-14-44	47.33	0.76	12.10	6.22	0.08	4.50	15.31	0.88	2.56	0.14	0.33	0.06
CZ. 80-720-161	45.36	0.79	13.10	6.97	0.11	5.86	17.57	0.85	2.13	0.27	0.20	0.04
CZ. 81-19-85	41.86	0.70	13.00	6.81	0.11	5.01	19.09	0.98	2.48	0.21	0.38	0.09
CZ. 80-14-42	44.21	0.73	12.40	6.63	0.10	4.56	16.83	1.14	2.40	0.43	3.78	0.06
CZ. 81-19-67	42.88	0.72	12.00	6.45	0.10	4.61	18.78	0.86	2.56	0.27	0.31	0.08
CZ. 81-588c-349	47.34	0.84	12.70	6.89	0.11	4.97	16.90	1.01	2.11	0.34	0.28	0.03
CZ. 80-16-6	44.28	0.63	12.00	5.94	0.10	5.92	18.56	1.19	1.59	0.25	0.26	0.05
CZ. 80-16-17	36.23	0.64	10.20	5.49	0.11	4.43	25.02	1.17	1.48	0.23	0.51	0.07
CZ. 81-588c-325	35.62	0.57	8.66	4.77	0.09	4.83	24.93	0.57	2.00	0.24	0.82	0.04
CZ. 81-653-182	46.50	1.13	13.90	7.41	0.13	6.73	33.00	2.02	1.91	0.20	0.66	0.16
CZ. 81-588c-254	51.60	0.80	13.70	6.77	0.12	6.11	24.10	0.71	2.71	0.33	0.88	0.08
CZ. 81-588c-510	51.90	0.77	12.50	6.95	0.12	5.90	23.10	0.72	2.65	0.28	0.68	0.08
CZ. 80-628-48	54.70	0.81	13.10	7.10	0.12	6.32	12.20	1.05	2.81	0.20	0.40	0.05
CZ. 80-725-282	38.20	0.63	10.37	6.11	0.12	4.81	20.30	0.67	2.81	0.28	0.44	0.06
CZ. 81-588c-306	47.10	0.70	11.13	6.01	0.11	5.70	24.30	0.60	2.32	0.28	0.77	0.04
CZ. 81-640-4	51.70	0.89	13.60	6.33	0.11	6.53	22.80	2.02	2.71	0.28	0.90	0.06
CZ. 80-640-56	46.30	0.78	12.80	6.88	0.12	6.60	16.50	1.97	1.78	0.20	0.26	0.16
CZ. 80-725-288	38.30	0.63	9.86	5.99	0.12	4.84	17.00	0.58	2.02	0.27	0.43	0.07
CZ. 80-725-306	36.90	0.62	9.15	5.83	0.11	4.74	17.00	0.57	2.01	0.26	0.43	0.06
CZ. 81-588c-338	43.90	0.67	9.45	5.48	0.11	5.50	30.20	0.52	2.33	0.29	1.13	0.04
CZ. 80-652-131	47.90	0.80	14.10	7.22	0.12	7.30	19.00	2.03	0.75	0.20	0.28	0.17
CZ. 81-724-61	52.00	0.81	14.00	7.11	0.11	6.69	15.30	1.48	1.84	0.18	0.15	0.05
CZ. 80-652-80	38.40	1.16	9.17	6.12	0.13	5.75	35.00	0.67	1.94	0.20	0.86	0.14
CZ. 80-14-36	45.30	0.87	11.50	6.68	0.10	5.47	25.50	0.84	2.28	0.29	0.79	0.06
CZ. 80-628-2	53.60	0.85	14.20	7.18	0.13	6.07	12.90	1.01	2.88	0.21	0.41	0.19
CZ. 81-15,2-7	42.80	0.71	12.60	6.70	0.10	5.56	21.40	1.09	2.46	0.19	5.98	0.20
CZ. 80-16-8	54.00	0.91	13.70	7.37	0.13	5.70	14.00	0.77	2.72	0.20	0.18	0.03
CZ. 81-588c-502	52.00	0.76	13.80	7.01	0.12	6.13	16.30	0.73	2.34	0.26	0.22	0.05
CZ. 81-14-12	47.30	0.80	13.00	6.83	0.12	5.79	18.40	2.01	3.18	0.31	1.37	0.72
CZ. 81-588c-382	45.80	0.80	12.00	6.84	0.12	5.74	23.40	0.67	2.81	0.34	0.89	0.09
CZ. 80-627-148	56.00	0.95	12.90	7.33	0.11	6.49	12.10	0.92	2.49	0.16	0.37	0.03
CZ. 80-725-437	37.80	0.64	9.55	5.95	0.12	4.75	19.00	0.58	2.22	0.28	0.45	0.06

Table 3. Continued ...

| Samples	Sr	Cr	Ni	Cu	Zn	Ba	Pb	Rb	Co	Y	Zr	Ce	Rh	Nb	Tb	Pd
						ppm										
CZ. 80-14-35	694	333	122	161	228	0	0	65	11	51	222	641	0	0	0	0
CZ. 81-653-175	941	388	111	251	260	0	0	22	7	53	222	781	0	0	0	0
CZ. 80-725-293	921	419	2	164	311	0	0	51	149	48	189	344	0	0	0	0
CZ. 80-14-44	0	418	24	321	588	0	0	65	170	52	228	311	0	0	131	71
CZ. 80-720-161	1050	522	651	111	361	670	0	48	151	50	198	321	0	0	0	0
CZ. 81-19-85	972	503	355	225	414	0	0	82	130	47	222	190	0	0	0	0
CZ. 80-14-42	610	411	544	184	215	0	0	63	140	55	186	416	0	0	0	0
CZ. 81-19-67	815	416	158	175	264	0	0	83	163	57	219	11	0	0	0	0
CZ. 81-588c-349	1090	225	177	186	118	110	0	73	147	52	200	412	0	0	0	0
CZ. 80-16-6	1340	331	188	163	990	0	0	88	166	52	231	22	0	0	188	66
CZ. 80-16-17	1040	466	261	183	164	0	0	79	165	54	222	11	0	0	0	0
CZ. 81-588c-325	1370	344	351	211	152	0	0	74	156	49	199	411	0	0	0	0
CZ. 81-653-182	1500	486	173	15	503	0	0	23	154	56	229	717	0	0	0	0
CZ. 81-588c-254	1200	421	149	183	133	0	0	84	160	52	198	412	0	0	0	0
CZ. 81-588c-510	988	399	145	181	129	0	0	7	165	53	200	411	0	0	122	0
CZ. 80-628-48	888	566	151	147	127	0	0	79	291	53	238	419	0	0	188	0
CZ. 80-725-282	822	371	98	153	177	0	0	61	139	44	181	388	0	0	0	0
CZ. 81-588c-306	997	391	147	16	141	0	0	75	131	52	202	311	0	0	0.011	0
CZ. 81-640-4	677	332	127	166	443	0	0	66	175	53	188	299	0	0	0	0
CZ. 80-640-56	798	418	111	148	125	0	0	22	158	53	205	222	0	0	0	0
CZ. 80-725-288	937	405	117	163	130	0	0	66	142	55	147	611	0	0	0	0
CZ. 80-725-306	877	336	99	150	151	0	0	61	97	45	92	221	0	0	0	0
CZ. 81-588c-338	1600	438	524	187	159	0	0	76	118	20	235	200	0	0	153	0
CZ. 80-652-131	805	421	199	147	143	0	0	23	174	40	207	339	0	0	0	0
CZ. 81-724-61	614	404	184	157	123	0	0	54	152	49	204	333	0	0	331	0
CZ. 80-652-80	180	507	128	180	557	0	0	23	8	57	231	774	0	0	0	0
CZ. 80-14-36	1530	453	131	173	244	0	0	66	130	50	231	761	0	0	0	0
CZ. 80-628-2	913	577	152	148	129	0	0	86	321	54	239	415	0	0	276	75
CZ. 81-15,2-7	1000	382	145	141	126	0	0	80	144	52	174	444	0	0	0	0
CZ. 80-16-8	663	484	147	184	189	0	0	89	167	56	224	221	0	0	275	68
CZ. 81-588c-502	744	388	155	153	134	0	0	74	159	52	192	313	0	0	0	0
CZ. 81-14-12	753	377	151	184	153	0	0	92	137	58	196	338	0	0	0	0
CZ. 81-588c-382	1220	433	154	182	175	163	0	74	159	53	200	413	0	0	111	81
CZ. 80-627-148	797	495	147	149	139	0	0	72	175	52	221	422	0	23	0	0
CZ. 80-725-437	889	396	111	157	112	0	0	62	137	54	131	0	0	0	0	0
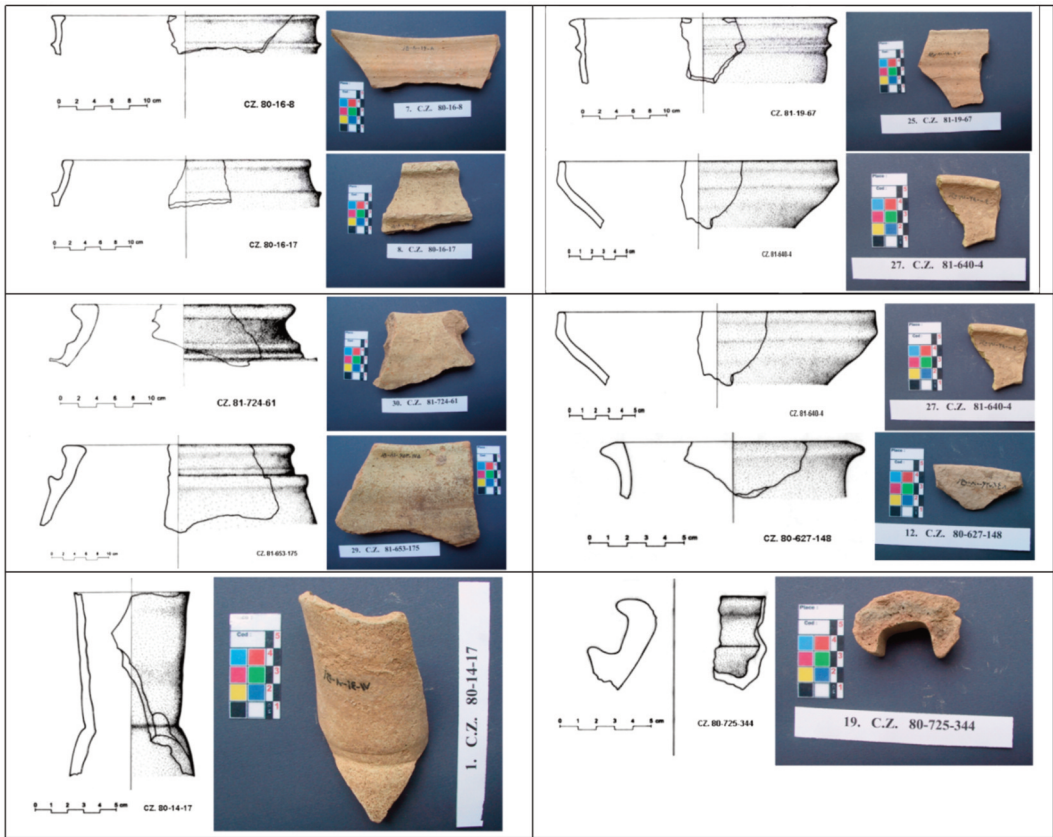
Figure 3. Some analysed samples with the number of the ceramic pieces.

parts of Mesopotamia (Noll, 1991). Calcium-rich ceramics are used for decorative features because of their bright surface and allow of surface modifications for aesthetic purposes. The character of the surface in calcium-rich ceramics increases the workability of the object, and it is employed for a better quality of surface decoration. Geological surveys in this area identified near Čoġā Zanbil alluvial soil setting, consisting mainly of calcareous material (Malek-Abbasi, 2004). The manufacturing process continued as a kind of non-continuous trade during the middle Elamite period.

Quantitative X-Ray Diffraction by Rietveld Refining Method

Phase determinations of pottery have been carried out by QXRD. The major crystalline phases in the matrix are calcite, quartz, feldspars, plagioclase and also high temperature phases such as pyroxene. The preferred orientations of common crystalline phases are shown in Figure 5. Quartz shows coarse grain aggregate, and is mostly used as admixture. The aggregates are well crystallized and the preferred orientation comes at $2\theta=26°$. Quartz become noticeable as crushed granite fragments and shows a different
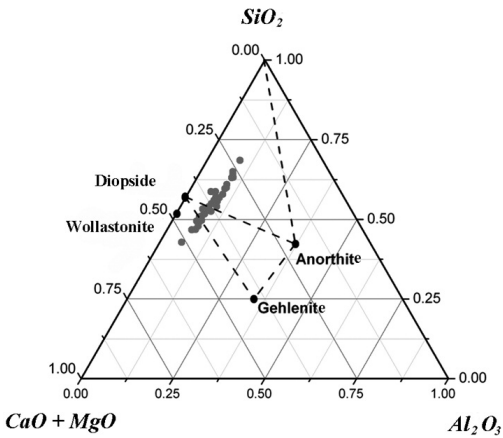
Figure 4. Bulk chemical composition of pottery with respect to calcium-silica constituents in the ternary system CaO+MgO-SiO$_2$-Al$_2$O$_3$ in wt%.

morphology as siliceous-igneous sources or clastic sedimentary rocks with influences of metamorphoses on their crystal structure, illustrated as typical undulatory extinction (Monnin et al., 2006). Granite fragments occur normally with alkali-feldspar, plagioclase, biotite and muscovite (Figure 6). Quartz shows a mostly rounded shape as result of the long transportation path from its original place. In general, in these groups the admixtures vary between crushed granite and sedimentary fragments. The variation of admixtures in the ceramic structure demonstrates that pottery makers would work with different materials to achieve a better quality production.

Calcite and iron oxide are used as flux or appear, after the firing process, as secondary
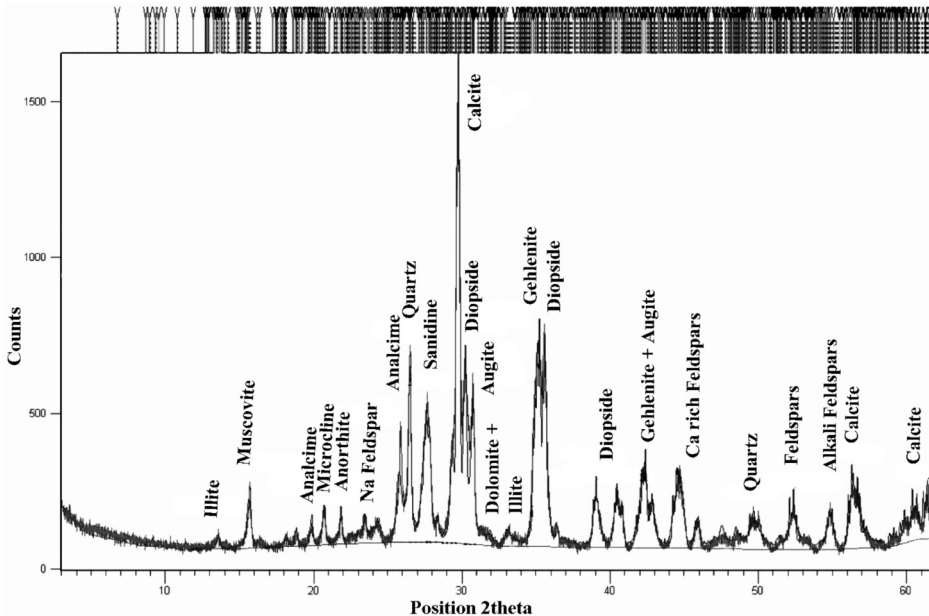
Figure 5. Diffractogram of one of the ceramics analyzed by XRD and refined by Rietveld calculation. Quartz- ICSD 79634, Calcite- ICSD 40544, Anorthite- ICSD 34942, Orthoclase- ICSD 34742, Albite- ICSD 87655, Microcline- ICSD 100495, Augite- ICSD 56921, Diopside- ICSD 64977, Muscovite- ICSD 202263, Dolomite- ICSD 40971, Illite- ICSD 55333, Gehlenite- ICSD 20392, Analcime- ICSD 87555.

crystallized phases in the matrix (Figure 7). The amount of Mg-rich carbonate proves that also dolomite is a common carbonate used as raw material. The enrichments of magnesium in carbonate - as dolomitic composition - can also be detected under polarized microscopy through the red rim remaining around calcium carbonate, responsible for the accumulation of periclase due to decomposition of dolomite: $CaMg(CO_3)_2 \rightarrow CaO + MgO + CO_2\uparrow$ by approximately 870 °C (Figure 7). In this condition one hypothesis says that periclase diffuses from the dolomite or high magnesium calcium carbonate, and some of it remains as red relic around the aggregate or porosity in the matrix. Alternatively, it could be a pore with secondary calcite formation. Gehlenite and pyroxene is mainly the reaction product from clayey raw material. Diopside occurs in Mg-rich matrix, rebuilt under high temperature conditions.

Because of the inhomogeneity of the ceramic constituents, all atomic and symmetry parameters have been refined through the Rietveld method to get a better matching in the structure of the calculated phases. Furthermore, all refined diffractograms have been compared to each other

to gain a better understanding of the crystalline phase constituents (Figure 8). The refining of some phases is difficult as they occur as very fine crystals, such as analcime (trigonal-rhombohedral), detected before quartz and overlapped with the best preferred orientation of quartz. Before the best peaks of quartz in 2θ=26°, Analcime ($Na[AlSi_2O_6]\cdot H_2O$) appeared based on weathering of albite and absence of 1 mole SiO_2 in its crystal structure in humid environment, accordingly (Deer et al., 1992). The qualitative phase investigation in this period proves that muscovite contains 1.4 wt% of the ceramic texture. Muscovite occurs with its best intensity on the plane (025) and its best preferred orientation at 2θ=13.5°. Muscovite is mostly overlapped by the major picks of quartz and diopside. Another imperative paragenesis in the pottery is due to the presence of the minerals carrying calcium and magnesium. Calcite, augite, diopside and gehlenite are the typical mineral in this group and the occurrences of the phases in a ceramic are dependent on the firing temperature, cooling rates and atmosphere of kiln (fCO_2) (Matson, 1971). The ceramics can be distinguished and sorted according to the
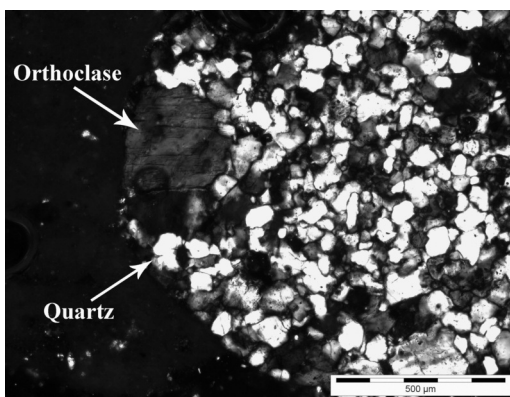

Figure 6. Granite fragments as quartz assembling with undolatory extinction. Quartz grain are cemented in a clay/calcareous matrix and form a very compact quartz mosaic
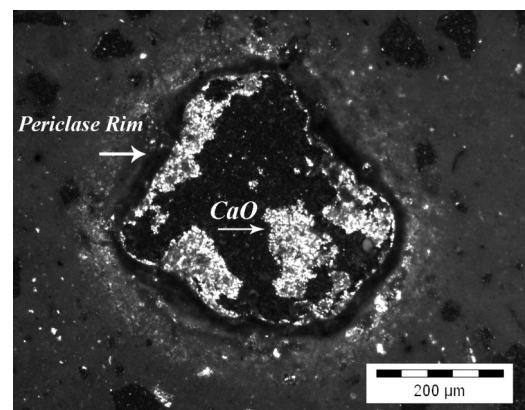

Figure 7. Diffusion and accumulation of periclase as relict of red rim on the external layer of carbonate after the dissolution of the dolomitic constituents.
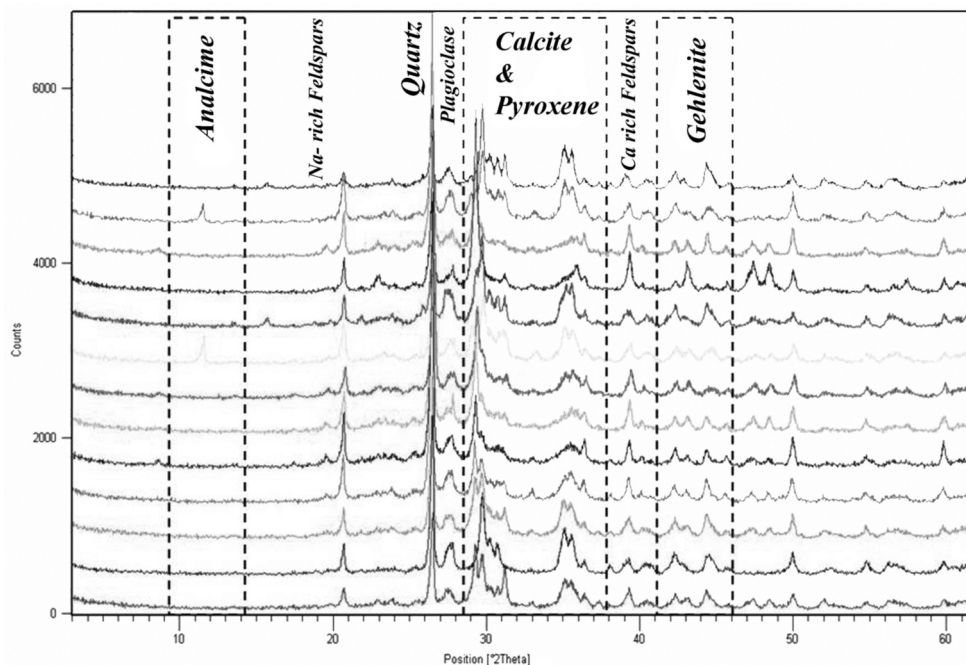
Figure 8. QXRD diffractograms refined by Rietveld method from Čoġā Zanbil (12th B.C.).

occurrence of Ca/Mg silicate. Consequently the gehlenite/pyroxene ratio has a great variation depending on the different soil, in which it is buried for a long time. The composition of plagioclases and feldspars varies with respect to the raw materials used in the manufacture. XRD analysis proved that the samples contain high amount of anorthite and K-feldspars (4.5 wt%) originating from the clay. The alteration processes of K-feldspars confirm that potteries from Čoġā Zanbil are made from an illite reservoir.

Phase decomposition by Simultaneous Thermo Analysis (STA)

The results based on STA-Analysis proved that the temperature reach approximately 1191 °C (Figure 9, Table 4). At this temperature, prolong firing goes to intensive smelting process due to the partial smelting between the surfaces of constituents clay grains (Traore et al., 2000; Rathossi et al., 2010). According to occurrences of hematite due to the oxidation of iron (II) to iron (III), it can be determined that the firing process has been carried out under oxidation conditions. The decomposition of carbonates (by 720-870 °C) is a reason for a different atmospheric condition in the kiln with respect to $f\mathrm{CO_2}$ (Emami et al., 2009). $f\mathrm{CO_2}$ increased because of the decomposition of calcite ($\mathrm{CaCO_3} \leftrightarrow \mathrm{CaO} + \mathrm{CO_2}\uparrow$). For a very short moment $f\mathrm{CO_2}$ increased in the kiln atmosphere and the reaction go to the left side. As a result, secondary calcites are produced in the porosity. This effect was enhanced through the influence of $\mathrm{CO_2}$ partial pressure on the kiln atmosphere as a closed system. The firing process has therefore been carried out in a short time in reduction conditions. The shifting of the
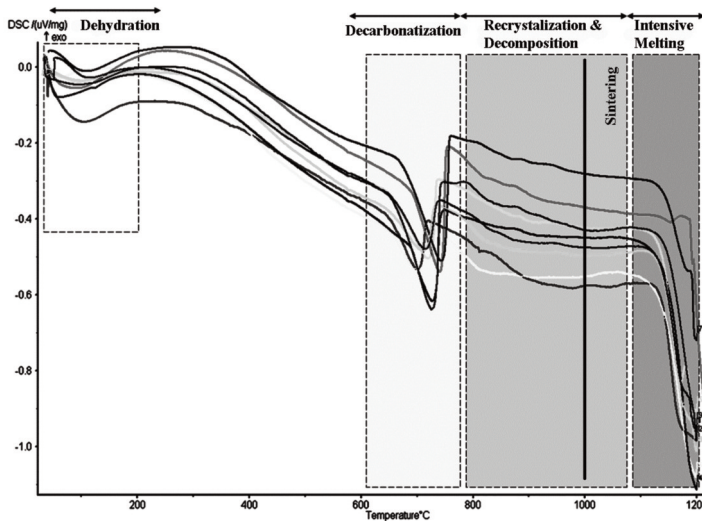
Figure 9. STA Diagram of the ceramics from 12th B.C. from Čoġā Zanbil.

Table 4. Mineral decomposition of the ceramics due to their temperature increasing in the kiln.

< 200 °C	Physical bonding water vanish
DSC Value 400-600 °C	Decomposition of kaolinite to metakaolinite $Al_2(OH)_4(Si_2O_5) \rightarrow Al_2O_3 \cdot 2SiO_2 + 2H_2O$
DSC Value 734-852 °C	Oxidation of impurities as well as decarbonisation
DSC Value 780-1000 °C	Emerging of spinels $2(Al_2O_3 \cdot 2SiO_2) \rightarrow 2Al_3O_3 \cdot 3SiO_2 + SiO_2$, additionaly Gehlenite and Pyroxene rebuilt in this area Secondary Iron oxide appeared
DSC Value 1000-1150 °C	Crystallization of spinelle from metakaolinite and emerge of Mullite $3Al_2O_3 + 6SiO_2 \rightarrow 3Al_2O_3 \cdot 2SiO_2 + 4SiO_2$
TG Mass Exchange	-4,5% (589-760 °C)

decarbonatization peak demonstrates that the atmospheric swap was controlled by CO_2 partial pressure in the kiln. After the STA-diagram and dehydration scope, the firing temperature is mainly constant and in this period the raw

material might have been illite rich clay.

Gehlenite is expected to have been crystallized in higher amount than clinopyroxene in low fired lamps (ca. 800 °C) (Traore et al., 2000). In lamps fired at temperature higher than 1000 °C or for

prolonged retention at the maximum temperature, the gelhenite content is expected to have been diminished as it is reacted with residual quartz towards anorthite and wollastonite (Rathossi et al., 2010), and therefore some high temperature phases are overlapped each other in XRD diagrams.

Mineralogical and petrological observations
The Matrix. The matrix of the objects might be classified based on grain size, fractional properties and porosity distribution in the samples (Emami and Trettin, 2010).

The matrix colour goes from green to bright green, because of chlorite, clinochlore and mainly diopside incidences. The matrix of the samples is compact and the porosity is reduced accordingly. The porosity in these structures is mainly secondary since they extended after firing. The difference between the textures of the ceramics can be discussed on the basis of occurrences of quartz – alkali feldspar – (± plagioclase) and mica. Iron and iron-components are mainly observed in the porosity of ceramics and they mostly cause the commonly observed red color of such objects (Maniatis and Tite, 1981). The occurrence of iron minerals such as hematite (Fe_2O_3) and goethite (FeOOH) proves that the iron rich phases generate through accumulation of colloidal iron rich components coming from the clayey resources. The accumulation of iron phases as hematite proves that the firing temperatures passed through a high oxidation reaction, as consequently hematite appear together with magnetite at a lower temperature (Pownceby and Clout, 2000). The recrystallization of hematite is also a reason for a high temperature reaction (Emami and Trettin, 2010).
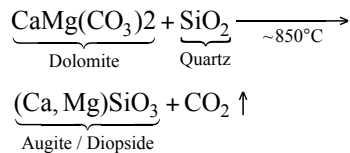
Mineralogical constituents
Petrological observations and investigations show that the objects consist of aggregates of granite and coarse grain sedimentary stone. Both consist of calcareous materials. In this group,

calcite is used as an admixture in the texture of ceramics and occurs either as primary or as secondary calcite. Furthermore, observations prove that the raw materials vary between calcitic and dolomitic compositions. According to the high constituents of calcareous and siliceous materials, an invariant reaction takes place, and leads to a heterogeneous material consisting of quartz and calcite, rebuilding a glassy and a pyroxene rich matrix. Increasing the Ca-containing minerals will increase the variation of pyroxenes, such as wollastonite, augite and diopside, in the matrix (Equation 1 and 2). The stability of such minerals depends on the alkali oxide/SiO_2 ratio. Pyroxene could therefore be a thermometer for the whole sintering reaction.

Equation 1

$$\underset{\text{Calcite}}{CaCO_3} + \underset{\text{Quartz}}{SiO_2} \xrightarrow{\sim 750°C} \underset{\text{Wollastonite}}{CaSiO_3} + CO_2 \uparrow$$

Equation 2

$$\underset{\text{Dolomite}}{CaMg(CO_3)2} + \underset{\text{Quartz}}{SiO_2} \xrightarrow{\sim 850°C}$$
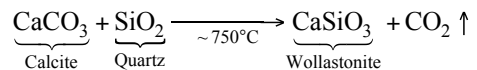
$$\underset{\text{Augite / Diopside}}{(Ca, Mg)SiO_3} + CO_2 \uparrow$$
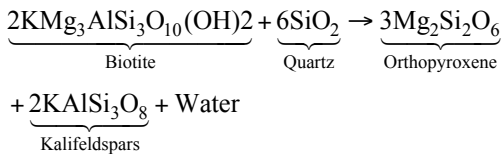
Plagioclases are the most common minerals in the matrix, and form tiny crystals approximately 50 µm to 1 mm in length. These aggregates are mostly prismatic with hypidiomorph to xenomorph morphology and they also grow along the (010) surface. They occur as post-deformation rebuilt crystals in the matrix from 800 °C. Plagioclases proved alteration effects on their surface as sericitization which proved the weathering condition in which the granitic resource was located (Figure 10). Alkali feldspars appeared mostly through exsolution of Na-lamellas on the orthoclase (optically is microcline) as reason for magmatic resource of

additions to the ceramic (Figure 11).

Biotite and muscovite are detectable through microscopic observations. Biotite originates from clayey raw materials as well as from corroded sediments. They can be detected through their red-brown color due to Fe^{2+}/Mg^{2+} to OH, their typical cleavage perpendicular to {001} surface and also their pleochroitic effect. Biotite decomposes through the firing process according to the dehydration reaction by 790 - 840 °C (Eq. 3); this reaction causes the formation of pertithic structure in biotite (Okrusch and Matthes, 2006).

Equation 3

$$\underbrace{2KMg_3AlSi_3O_{10}(OH)2}_{\text{Biotite}} + \underbrace{6SiO_2}_{\text{Quartz}} \rightarrow \underbrace{3Mg_2Si_2O_6}_{\text{Orthopyroxene}}$$

$$+ \underbrace{2KAlSi_3O_8}_{\text{Kalifeldspars}} + \text{Water}$$

The existence of diopside and alkali feldspars in the matrix leads to estimate the firing temperature to around 950 °C < T < 1100 °C, then the alkali feldspars are molten by higher temperatures. According to the mineralogical system $NaAlSi_3O_8$ - $KalSi_3O_8$ - SiO_2 it seems that the stability area stands in the feldspar -

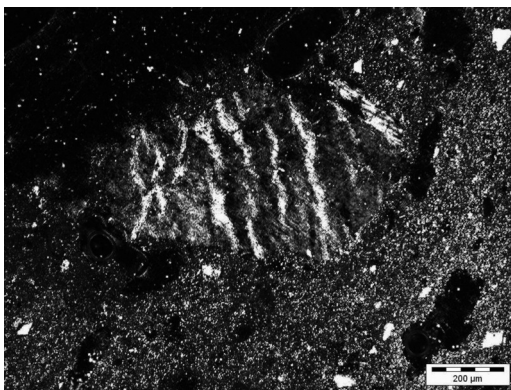tridymite area and therefore the sinter temperature must not be higher than 1100 °C.

Concluding remarks

Mineralogical-chemical investigations on ceramics from Čoġā Zanbil (12th B.C.) allow useful interpretations regarding the manufacture of pottery in this area. Based on petrographical observations, the materials used for pottering in Čoġā Zanbil seem to have sedimentary origins with some metamorphic influences.

The chemical composition and the calculated crystalline phase constituents in the body of ceramics are in the system SiO_2 - Al_2O_3 - $(CaO+Na_2O+K_2O)$ - $(MgO+\Sigma Fe_xO_y)$ (Figure 12). The segregated part from the tetrahedral diagram shows CaO-rich materials as calcareous raw material used in the ceramic production. K_2O and CaO as flux are among them, and the sinter temperatures, based on the stability field of these phases, decreased. The prolong temperature reaction also caused the crystallization of pseudo-mullite as a reason for partial smelting at temperature between 1000 to 1100 °C. The common minerals paragenesis showed as follow:
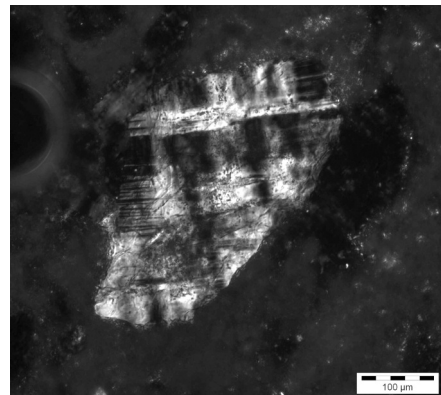
1) Anorthite - Calcite - Diopside

Figure 10. Sericitization on plagioclase as a result of weathering reactions.

Figure 11. Na-lamellas as exsolution relicts on orthoclase.
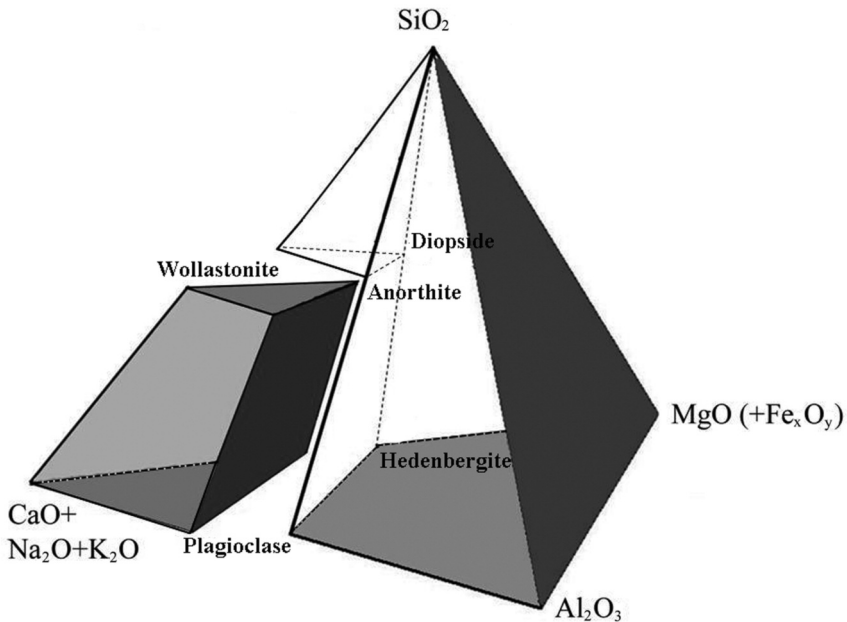
Figure 12. Mineral paragenesis in the ceramics from Čoġā Zanbil in tetrahedral diagram SiO_2 - Al_2O_3 - $(CaO+Na_2O+K_2O)$ - $(MgO+\Sigma Fe_xO_y)$.

2) Gehlenite - Augite - Diopside - Ca-plagioclase

3) Anorthite – Diopside

Clustering of phase constituents (by QXRD) shows that the technology used here varied depending on the raw material and the admixtures. The matrix consists of iron-rich clay, well processed and manufactured under oxidation reaction. The pottery technology in this area shows a few changes and the technology remained constant. The atmosphere of the kiln changed because of the shifting of the calcite decomposition peak range and the recrystallization peaks by 800 °C to 900 °C. The new crystallization of wollastonite, diopside and anorthite through residual quartz allow the supposition that the sinter took place under 1000 °C (ca 950 °C), but due to the absence of high temperature phases such as mullite, the reaction continues as partial smelting instead of firing. Different ceramic processing was carried out in Čoġā Zanbil with dissimilar firing conditions, with similar raw materials and admixtures as filler in the pottery. Firing process divided in two groups: sintered ceramics and intensive smelted ceramics

References

Adams R.M. (1962) - Agriculture and urban life in early southwestern Iran. *Science*, 136, 109-122

Bullard R. G. (1970) - Geological Studies in Field Archaeology. *Biblical Archaeologist*, 33, 98-132.

Deer W.A., Howie R.A. and Zusmann J. (1992) - An

introduction to the rock-forming mineral, 3rd Edition, Longman Scientific & Technical.

Drebushchak V.A., Mylnikova L.N. and Drebushchak T.N. (2011) - The mass-loss diagram for the ancient ceramics. *Journal of Thermal Analysis and Calorimetry*, 104, 459-466.

Emami M. A. (1996) - Relation of Geological Surveys with Pathology of Historical Materials and Ambits (Geoarcheology of Choghazanbil Temple). *Proceedings of 1th Symposium on Reservation and Restoration of Historical- Cultural Heritages* (455-465). Tehran: Research Center of Conservation and Restoration of Cultural Heritage.

Emami M.A. (2008) - "*Mineralogisch chemische Untersuchungen zur Archaeometrie elamischer Keramiken aus Khousestan, Iran*", Dissertation, Universitaet Siegen, URN: nbn: hbz: 467-3603

Emami M. A. and Trettin R. (2010) - Phase generating processes in ancient ceramic matrices through microstructure investigation with high resolution microscopy methods. *Journal of Advanced Microscopy Research*, 5(11), 181-189.

Emami M., Kowald, T. and Trettin R. (2009) - Mineralogical and chemical investigation on the recrystallization process during sintering in face-interface areas in ancient ceramic matrices. *Materials and Manufacturing Process*, 24, 934-941.

Emami M., Volkmar J., and Trettin R. (2008) - Quantitative characterization of damage mechanisms in ancient ceramic by quantitative X-ray powder diffraction, polarization microscopy, confocal laser scanning microscopy and non-contact mode atomic force microscopy. *Surface Enginnering*, 24, 129-137.

Emami M., Volkmar J. and Trettin R. (2011) - Characterization of Ancient Ceramic Matrices with High Resolution Microscopy Methods, Laser Scanning, Theory and Applications, Prof. Chau-Chang Wang (Ed.), ISBN: 978-953-307-205-0, InTech.

Fesharaki O., García-Romero E. Cuevas-González J. and López-Martínez N. (2007) - Clay mineral genesis and chemical evolution in the Miocene sediments of Somosaguas, Madrid Basin, Spain. *Clay Minerals, 42(2)*, 187-201.

Gasparik T. (1990) - A thermodynamic model for the enstatite-diopside join. *American Mineralogist*, 75, 1080-1091.

Ghirshman R. (1968) - *Tchoga Zanbil (Dur Untash),*

Vol. II. Temenos, temples, palais, tombes. Paris: Memories de la delegation archaeologique en Iran 40.

Gradstein F.M., Ogg J.G. and Smith A.G. (2004) - A Geologic Time Scale. *Cambridge University Press, and the official website of the International Commission on Stratigraphy (ICS) under* www.stratigraphy.org.

Heimann R. B. (1978) - Mineralogische Vorgaenge beim Brennen von Keramik und Aechaeothermometrie. *Acta Prehistorica et archaeologica*, 9, 10, 79-101.

Kambakhsh Fard S. O. (2001) - *Pottery in Iran, from Neilithic Period to the Present.* Tehran, Iran: Qoqnoos Publishing.

LeChatelier H. (1912) - Note sur la matiere noire et bitumineuse de certains reliefs et statuettes. *Mermories de la delegation en Perse XIII*, pp. 162.

Louër D., and Louër M. (1972) - Méthode d'essais et erreurs pour l'indexation automatique des diagrammes des poudre. *Journal of Applied Crystallography*, 5, 271-275.

Magetti M., and Gelatti G. (1982) - Die refernzgroupe(n) Lousana-mineralogische und chemische Untersuchungen der keramischen Produktion der Toepferwerkstaette Berna. *Jahresbericht der schweizerichen Gesellschaft fuer Ur- und Fruehgeschichte, 65*, 109-132.

Maggetti M., and Schwab H. (1982) - Iron age fine pottery from Chatillon-s-Glane and the Heuneburg. *Archaeometry*, 24, 21-36.

Maggetti M., Neururer Ch. and Ramseyer D. (2011) - Temperature evolution inside a pot during experimental surface (bonfire) firing. *Applied Clay Science*, 53, 500-508.

Malek-Abbasi A., (2004) - Chogha Zanbil survived, but why?, *32th International Geological Congress, Italy, Florence.*

Maniatis Y., and Tite M.S. (1981) - Technological examination of neolithic-bronze age pottery from central and southeast Europe and from the Near East. *Journal of Archaeological Research*, 8, 59-76.

Martineau R., Walter-Simonnet A.V., Grobety B. and Bautier M. (2007) - Clay resources and technical choices for Neolithic pottery (Chalian, Jura, France), chemical. mineralogical and grain-size analysis. *Archaeometry*, 49, 23-52.

Matson F. (1971) - A study of temperatures using in firing ancient Mesopotamian pottery. In R.H. Brill, *Science and Archaeology* (pp. 65-79). M.I.T. Press,

Cambridge.

Mofidi Nasrabadi B. (2003) - Untersuchungen zu Siedlungsstrukturen an der Peripherie von Tschogha Zanbil (Dur Untasch). *Archäologischer mitteilungen aus Iran und Turan (AMIT), 35-36*, 241-265.

Monnin Y., Degrugilliers P., Butleed D. and Garcia-Diaz E. (2006) - Petrography of two siliceous limestone's submitted to alkali-silica reaction. *Cement and Concrete Research* , 36, 1460-1466.

Negahban E.O. (1991) - *Excavation at Haft Tape. Iran.* University Monograph 70, Philadelphia.

Noll W. (1991) - *Alte Keramiken und ihre Pigmente, Studien zu Material und Technologie.* D-7000 Stuttgart: E. Schweizerbart'sche Verlagsbuch handlung.

Okrusch M. and Matthes S. (2006) - *Mineralogie.* Germany: 9. Auflage, Springer Verlag, Berlin-Heidelberg-New York.

Oudbashi O. and Emami M. (2010) - A note on corrosion morphology on some midlle elamite copper aloy artefacts from Haft-Tappeh, south-west Iran. *Studies in Conservation*, 55, 20-25.

Potts D. (1999) - *The Archaeology of Elam:Firmation and Transformation of an Ancient Iranian State.* Cambridge: Cambridge University Press.

Pownceby M.I. and Clout M.F. (2000) - Phase relation in the Fe-rich part of the system Fe_2O_3-Fe_3O_4-CaO-SiO_2. *Mineral Process and Extractive Metallurgy*, 109, 36-48.

Rathossi C., Pontikes Y. and Tsolis-Katagas P. (2010) - Mineralogical differences between ancient sherds and experimental ceramics: Indices for firing conditions and post- burial alteration. Bulletin of the Geological Society of Greece, 2010, Proceedings of the 12th International Congress, Greece, Patras, May, 2010.

Salmang H. and Scholze H. (1983) - *Keramik, Teil 2. Keramische Werkstoffe.* 6. Auflage, Springer Verlag, Berlin, Heidelber, New York.

Szilágyi V., Gyarmati J., Tóth M., Taubald H., Balla M., Kasztovszky Zs. and Szakmány Gy. (2012) - Petro-mineralogy and geochemistry as tools of provenance analysis on archaeological pottery: Study of Inka Period ceramics from Paria, Bolivia. *Journal of South American Earth Sciences*, 36, 1-17.

Stoeklin J. (1968) - Salt deposits of the middle east. In R. B. Edited Mattox. *International Conference on Saline Deposits* (88, 158-181). Houston, Texas: Geological Society of America.

Sumner W. (1972) - *Cultural Development in the Kur River Basin, Iran; An archaeological Analysis of Settlement Patterns.* Philadelphia: Ph.D. Thesis, Departement of Anthropology, University of Pennsylvania .

Tehrani K. (1989) - *Stratigraphy of Iran and Type Sections of Formations.* Tehran: Tehran University Publication.

Traore K., Kabre T.S., and Blanchart P. (2000) - Low temperature sintering of a pottery clay from Burkina Faso. *Applied Clay Science* 17, 279-292.

Van der Voo R. (1993) - Paleomagnetism of the Atlantic, Tethys and Lapetus ocean, Cambridge University Press.

Wong H.S. and Buenfeld N.R. (2006) - Euclidean distance mapping for computing microstructural gradients at interfaces in composite materials. *Cement and Concrete Research*, 36, 1091-1097.